

Electronic Supporting Information (ESI)

Lysine and Dithiothreitol Promoted Ultrasensitive Optical and Colorimetric Detection of Mercury Using Anisotropic Gold Nanoparticles

Abhishek Chaudhary[‡], Charu Dwivedi^{‡*}, Mohit Chawla, Abhishek Gupta, Chayan K. Nandi*

School of Basic Science, Indian Institute of Technology Mandi, Mandi-175001, India

e-mail: charudwived@gmail.com; chayan@iitmandi.ac.in

1. Material and Methods

1.1 Materials

All glassware were washed with aqua regia (3 HCl: 1 HNO₃), followed by rinsing with double distilled water for several times. All the chemicals gold (III) chloride hydrate (HAuCl₄.3H₂O 99.99%), potassium iodide (KI (> 99)), L-ascorbic acid, dithiothreitol (DTT) sodium borohydride (NaBH₄, 99%), and silver nitrate (AgNO₃, 99.5%), lysine, cysteine, aspartic acid, tryptophan, proline, tyrosine and alanine were purchased from Sigma Aldrich. Hexadecyltrimethyl-ammonium chloride (CTAC, >95%), sodium citrate tribasic hydrate (> 99%), N-Cetyl-N,N,N-trimethyl-ammonium bromide (CTAB), sodium hydroxide pellet purified (NaOH, 97%), sodium arsenite, and chloride salts of lead, mercury, chromium, cadmium, magnesium, barium, nickel, manganese and zinc, with purity >99%, were purchased from Merck. Double distilled 18.3 mΩ deionized water (Elga Pure lab Ultra) was used throughout the preparation of solutions.

1.2 Synthesis of anisotropic gold nanoparticles

The anisotropic gold nanoparticles were synthesized in the seedless synthesis method developed by Chen et al.^[1] In brief, 0.1 M CTAC (1.6 ml) was first diluted with 8 mL of ultrapure water, and subsequently 0.01 M KI (75 μL), 25.4 mM HAuCl₄.3H₂O (80 μL) and 0.1 M NaOH (20.3 μL) were added into this solution in the same order yielding a light yellowish color solution. 0.064M ascorbic acid (80 μL) was added to this solution with mild stirring followed by fast injection of 0.1 M NaOH (10 μL) and this solution was left undisturbed for 15 minutes. This resulted in a blue suspension. The extra CTAC was removed by centrifugation and the pellet obtained was resuspended in the equal amount of water. The concentration of the nanoparticles was calculated by assuming that all the HAuCl₄.3H₂O have been converted to nanoparticles and the concentration of anisotropic GNP was determined to be 6.1 nM.^[2]

1.3 Synthesis of spherical gold nanoparticles

CTAB stabilized spherical GNP were synthesized by using a seed-mediated growth method.^[3] The container for seed synthesis contained 5 mL of 0.50 mM HAuCl₄.3H₂O and 5 mL of 0.20 M CTAB. The solution was reduced by addition of 650 μL of ice-cold NaBH₄ (0.010 M) followed by vigorous stirring for 2 min. The seed solution was aged for 2 hours before use. 20 μL of seed solution was added to a solution containing 9.50 mL of 0.10 M CTAB, 80 μL of 0.010 M AgNO₃, 500 μL of 0.010 M HAuCl₄.3H₂O and 65 μL of 0.10 M ascorbic Acid. The resulting mixture was stirred for 10 min and a red suspension was obtained which was kept undisturbed overnight. The extra CTAB was removed by centrifuging the nanoparticles twice at 10000 rpm, for 10 min and the pellet was re-suspended in the equal amount of water and stored for further use. The average size of the synthesized spherical nanoparticles is ~20 nm.

1.4 Characterization of the gold nanoparticles

Particle size and dispersity of the synthesized nanoparticles were characterized by using a TECNAI 200 kV TEM (FEI, Electron Optics). 1 ml of as synthesized anisotropic and spherical GNP solutions were centrifuged and washed twice with double distilled water and the pellet obtained was re-suspended in 20 μ L of water to concentrate the samples before TEM analysis. However, GNPs/Hg⁰/Lys, GNPs/Hg⁰/Lys/DTT and spherical GNP/Hg⁰/Lys/DTT sample were used as it is without changing the concentration. Fast Fourier transform (FFT) analysis was done from selected area of the HRTEM image of the edge of GNP, which has been enclosed by the white box in the image. The lattice images were constructed by the selective masking of the spots obtained from the FFT analysis of the area enclosed in the white box. UV-vis absorption spectra were recorded on Shimadzu Spectrophotometer. The DLS hydrodynamic radius of the nanoparticles were measured by using Zeta Sizer Nano, equipped with a He-Ne laser illumination at 633 nm in a single photon counting mode using avalanche photodiode for signal detection (Malvern Instrument). XRD diffraction patterns were recorded on Rigaku Smart Lab X-Ray diffractometer using Cu K α radiation as X-ray source ($\lambda=1.5418 \text{ \AA}$) at room temperature. The voltage and current for the measurement were kept 45 kV and 100 mA respectively.

1.5 Sample Preparation

The synthesized anisotropic nanoparticles were centrifuged twice at 10,000 rpm for 10 min and re-suspended in the same volume of double distilled water. For sensing of Hg²⁺ ions, 20 μ L of metal salt solution with appropriate concentration was equilibrated with the GNP solution (600 μ L of 6.1 nM,) for 15 min. To this solution 20 μ L of Lysine (14.5 μ M) and 20 μ L DTT (16 μ M) were added, respectively. The sample solutions were equilibrated at ambient temperature for the optimum incubation time, and, then the UV-vis absorption spectra of the solutions were recorded. The application of the developed assay was tested on the drinking water sample (collected from Indian Institute of Technology Mandi campus), after “spiking” the samples with standard solutions of Hg²⁺ (0.01-50 nM). The colorimetric assay was performed on these real samples as described earlier.

Table S1: Comparison of the detection limit using different nanoparticle-based probes for Hg²⁺ detection.

S.N.	Methods	Detection limit	Ref.
1.	Oligonucleotide–gold-nanoparticle hybrids	1.0 nM	[4]
2.	γ -Cyclodextrin-protected gold nanoparticles	49 .0 pM	[5]
3.	DNA-functionalized gold nanoparticle	25.0 nM	[6]
4.	Oligonucleotide functionalized gold nanoparticles	50.0 pM	[7]
5.	Aptamers-modified gold nanoparticles	30.0 pM	[8]
6.	Citrate capped gold nanoparticles	50 .0 nM	[9]
7.	Oligonucleotide functionalized gold nanoparticles	0.5 nM	[10]
8.	Gold nano rods	3.0 ppt	[11]

9.	Gold nano rods	0.1 pM	[12]
10.	Carbon nano dots	4.2 nM	[13]
11.	Spherical gold nanoparticles	2.0 ppb	[14]
12.	Gold nanorods	6.6×10^{-13} g/L	[15]
13.	Lysozyme Type VI-stabilized gold nanoclusters	3.0 pM	[16]
14.	Gold nano rods	2.4 pM	[17]
15.	DNA-functionalized gold nanoparticle	1.0 pM	[18]
16.	Anisotropic gold nanoparticles	27.0 pM	Present work

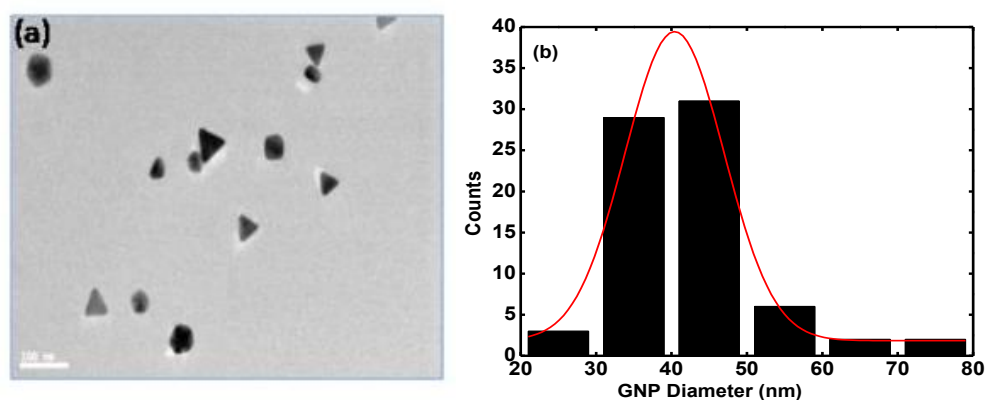


Figure S1: (a) TEM image and (b) size distribution histogram of the synthesized anisotropic GNP.

To confirm the Hg^0 -Au amalgamation, the XRD analysis of the GNP before and after Hg^0 adsorption is carried out. The XRD pattern (Figure S2, b) of GNP before the exposition to Hg^0 exhibits the peaks at 38.2° , 44.3° , 64.7° and 77.6° corresponding to (111), (220), (220) and (311) planes of gold, respectively.¹⁹ The high intensity peak at 38.2° , (111) plane, corresponds to the preferred orientation for polycrystalline FCC (face-centered cubic) metals deposited onto amorphous substrates. As the gold content of the sample is quite low, the intensity of the rest of the peaks is also relatively low. After Hg^0 adsorption also no major changes in the XRD pattern of the GNP is observed as the relative content of the Hg^0 in the sample is even less than gold. However, a small peak at 40.7° is observed in the XRD pattern of GNP- Hg^0 , corresponding to Au_3Hg , as reported in the literature.^[19-20]

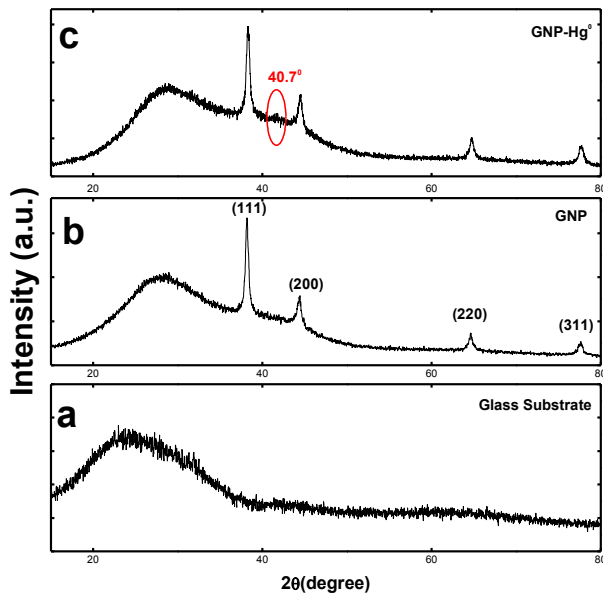


Figure S2: X-ray diffraction patterns of (a) glass substrate and GNP deposited on glass substrate (b) in the absence of Hg^0 and (c) in the presence Hg^0 .

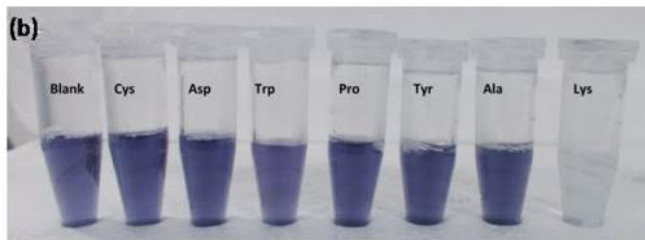
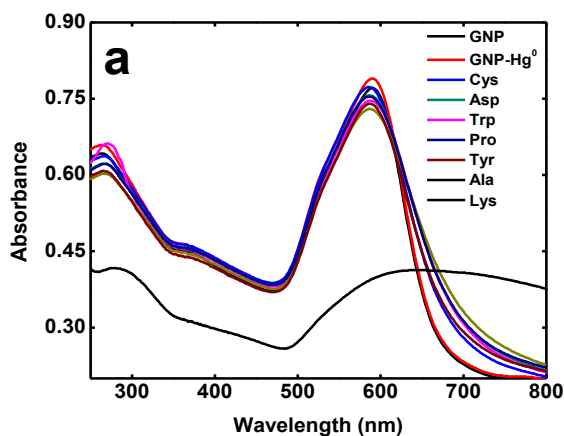


Figure S3: Effect of amino acids on the UV-vis spectra of the sensing system. SPR spectra of the colorimetric assay tested with 7 different amino acids, keeping concentration of Hg^0 and DTT 30nM & 16 μM respectively. (Cys: cysteine, Asp: aspartic acid, Trp: tryptophan, Pro: Proline, Tyr: tyrosine, Ala: Alanine, Lys: Lysine) (b) change in the color of GNP/ Hg^0 /DTT system in the presence of different amino acids. Blue to colorless color transition can only be seen in presence of Lys due to aggregation of GNP.

The effect of Lys concentration (2.8-14.25 μM) is studied by keeping concentration of DTT constant (**Figure S 4a**). It was observed that the upto 8.5 μM of Lys concentration, there is only slight decrease in the absorption intensity indicating binding of Lys with GNP. But at higher

concentrations, a significant decrease in absorption intensity is also accompanied with red shift of 13 nm in the SPR band at 590 nm. Therefore, 8.5 μM Lys is chosen as the optimized concentration. Furthermore, the effect of time on the SPR of GNP-Hg⁰-Lys system is also studied and it is observed that even after 2 h, no considerable shift or reduction in the SPR of GNP takes place (**Figure S 4b**). These results suggest that the optimized concentration of the Lys (8.5 μM) is not sufficient enough to generate colorimetric response when Hg⁰, DTT or both are absent. This observation is also supported by TEM analysis of the GNP-Hg⁰-Lys in which no aggregation is observed even after 2 h of contact time (**Figure S 5**).

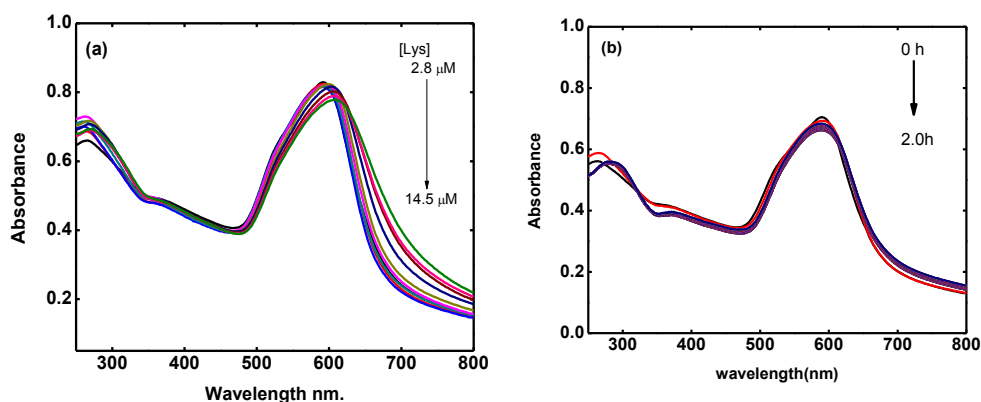


Figure S4: Change in the SPR of anisotropic GNP (a) in presence of different concentration of Lys (2.8 – 14.5 μM) and (b) with time at [Lys] = 8.5 μM . No significant change is observed in the SPR band at 590 nm upto 8.5 μM of Lys.

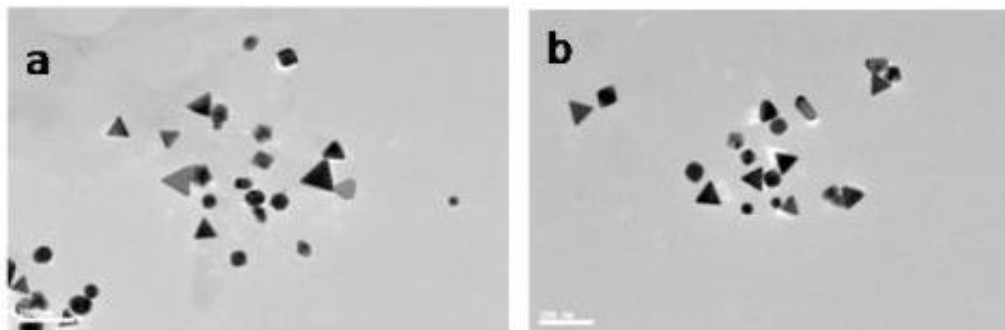


Figure S5: (a) and (b) TEM image of anisotropic GNP/Hg⁰/Lys system after 2 h of contact time. TEM image depicts that there is no significant agglomeration in the GNP/Hg⁰/Lys system in the absence of DTT.

The effect of the concentration of DTT is also checked by varying it from 0.5-20.0 μM at constant concentration of Lys (8.5 μM) in the absence of Hg⁰. A red shift of only 5 nm with 4% decrement in absorption intensity is observed in GNP-Lys system at highest concentration (50.0 μM) of DTT used (Figure S 6a.). On the basis of this experiment, the concentration of DTT was optimized as 16.0 μM . The effect of time on the particle stability in the presence of Lys and DTT

is also checked spectro-photometrically (**Figure S 6b**). No significant change in the peak position and intensity of the SPR band at 590 nm is observed even after 2 h of equilibration and hence the possibility of DTT induced aggregation, at the optimized concentration, is overruled.

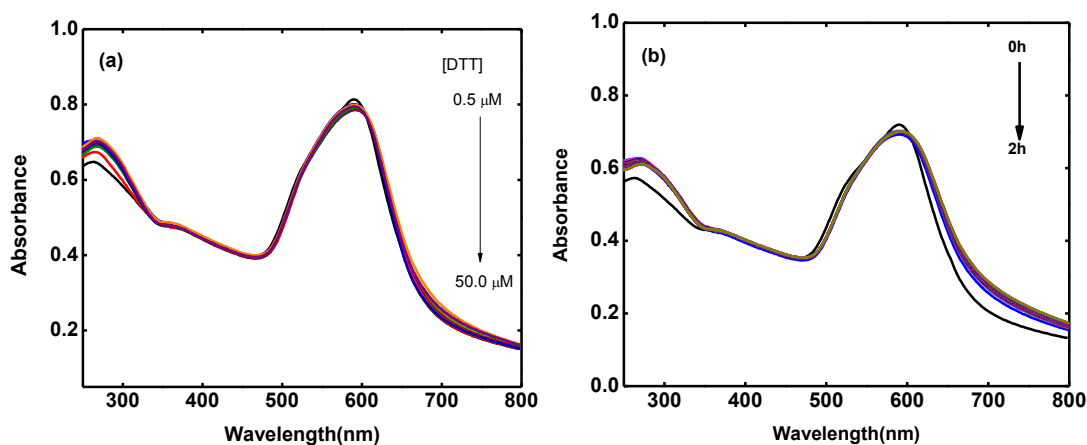


Figure S6: Change in the SPR of anisotropic GNP (a) in the presence of different concentration of DTT (0.5 μM-50.0 μM) and (b) with time at [DTT] =16.0 μM and [Lys] = 8.5 μM. No significant change is observed in the SPR band at 590 nm upto 16.0 μM of DTT.

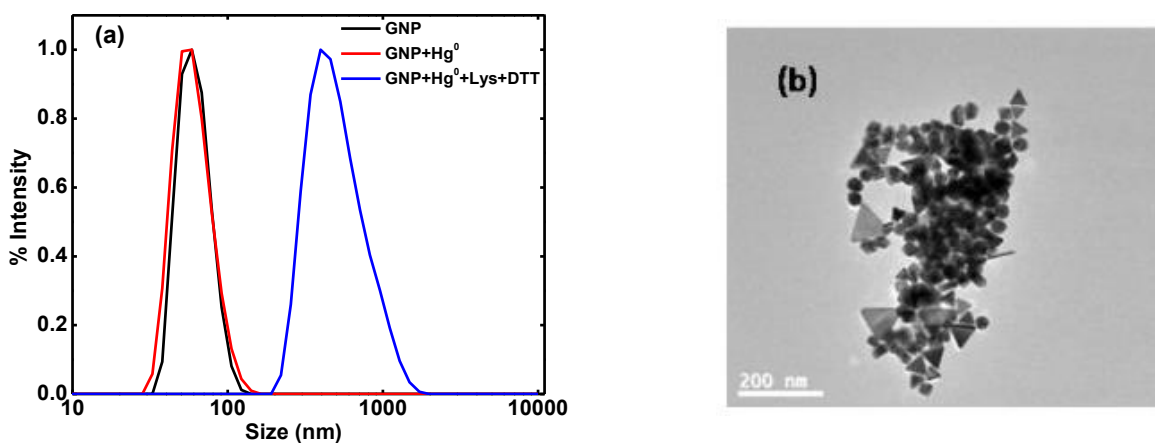


Figure S7: (a) Hydrodynamic size of the GNP, GNP/Hg⁰, and GNP/Hg⁰/Lys/DTT (b) TEM image of GNP/Hg⁰/Lys/DTT showing aggregation of the sensing system on addition of DTT.

The applicability of the developed colorimetric assay to real samples is evaluated by spiking tap water (sampled from IIT Mandi, India) with Hg²⁺ ions. The data on the physical and chemical examination of the tap water was provided by water testing lab of Irrigation & Public Health Department, Mandi, India. The water samples were collected in December, 2014

Table S2: Physicochemical properties of the tap water of Mandi, India.

Physicochemical property	Experimental value
Turbidity (NTU)	0.00 NTU
Conductivity (μS)	34.80 μS
Total dissolved solid	150.00 ppm
pH	7.79
Alkalinity	64.00 mg/L
Total hardness as CaCO_3	240.00 mg/L
Ca^{2+}	64.00 mg/L
Mg^{2+}	19.50 mg/L
Na^+	11.30 mg/L
K^+	5.30 mg/L
Cl^-	19.88 mg/L
SO_4^{2-}	2.80 mg/L
HCO_3^-	64.00 mg/l
F^-	0.35 mg/L

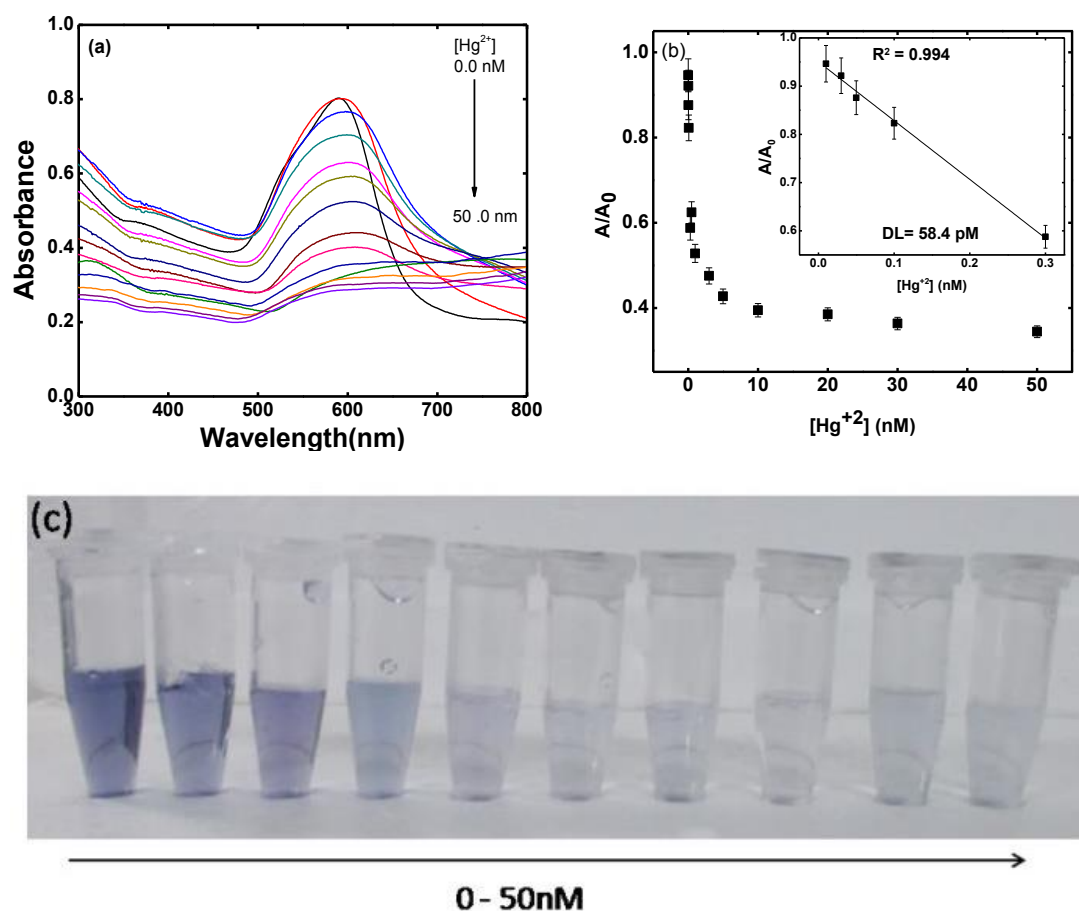


Figure S8: (a) UV-vis spectra of GNP/ Hg^0 /Lys/DTT system equilibrated for 15 min, with different concentrations of Hg^{2+} ions (0.01 nM-50.0 nM) in tap water (b) change in absorption intensity at 590 nm with change in concentration of Hg^{2+} ions, each data point is presented as

standard deviation from three replicate assays (c) change in the color of the GNP/Hg⁰/Lys/DTT system with different Hg²⁺ concentration in left to right order, 0-50.0 nM.

References:

1. L. Chen, F. Ji, Y. Xu, L. He, Y. Mi, F. Bao, B. Sun, X. Zhang and Q. Zhang, *Nano Lett.*, 2014, **14**, 7201.
2. D. J. Lewis, T. M. Day, J. V MacPherson and Z. Pikramenou, *Chem. Commun.* 2006, 1433.
3. R. Narayanan, R. J. Lipert and M. D. Porter, *Anal. Chem.* 2008, **80**, 2265.
4. D. Li, A. Wieckowska and I. Willner, *Angew. Chem. Int. Ed.* 2008, **47**, 3927.
5. M. C. Paa, C. K. Lo, X. Yang and M. F. M. Choi, *J. Phys. Chem. C*, 2010, **114**, 15995.
6. C. W. Liu, C. C. Huang and H. T. Chang, *Langmuir*. 2008, **24**, 8346.
7. S. Cai, K. Lao, C. Lau and J. Lu, *Anal. Chem.* 2011, **83**, 9702.
8. Z. Jiang, Y. Fan, M. Chen, A. Liang, X. Liao, G. Wen, X. Shen, X. He, H. Pan and H. Jiang, *Anal. Chem.* 2009, **81**, 5439.
9. G. H. Chen, W. Y. Chen, Y. C. Yen, C. W. Wang, H. T. Chang, and C. F. Chen, *Anal. Chem.* 2014, **86**, 6843.
10. Z. Zhu, Y. Su, J. Li, D. Li, J. Zhang, S. Song, Y. Zhao, G. Li and C. Fan, *Anal. Chem.* 2009, **81**, 7660.
11. T. Placido, G. Aragay, J. Pons, R. Comparelli, M. L. Curri and A. Merkoçi, *ACS Appl. Mater. Interfaces*, 2013, **5**, 1084.
12. H. Huang, C. Qu, X. Liu, S. Huang, Z. Xu, Y. Zhu and P. K. Chu, *Chem. Commun.* 2011, **47**, 6897.
13. L. Zhou, Y. Lin, Z. Huang, J. Ren and X. Qu, *Chem. Commun.*, 2012, **48**, 1147.
14. C. C. Huang and H. T. Chang, *Anal. Chem.* 2006, **78**, 8332.
15. M. Rex, F.E. Hernandez and A. D. Campiglia, *Anal. Chem.* 2006, **78**, 445.
16. Y. H. Lin and W. L. Tseng, *Anal. Chem.* 2010, **82**, 9194.
17. G. C. Yan, J. L. Wang, J. Deng and C. X. Zhang, *Chem. Commun.*, 2011, **47**, 12500.
18. J. Chen, S. Zhou and J. Wen, *Anal. Chem.* 2014, **86**, 3108.

19. D. Ballester, C. Gómez-Giménez, E. García-Díez, R. Juan, B. Rubio and M. T. Izquierdo, *J. Hazard. Mat.* 2013, **260**, 247.
20. T. Kobiela, Z. Kaszkar and R. Duś, *Thin Solid Films*, 2005, **478**, 152.